Response to Referee #2

We gratefully appreciate the reviewer for the careful reading of our manuscript and for the very constructive comments. We were able to enhance the scientific quality of our manuscript by incorporating the reviewer's comments and suggestions. Below, the reviewer's text is given in black while our replies and descriptions on how the comments have been addressed in the manuscript are given in blue.

The authors describe a new algorithm to retrieve NO_2 from the GEMS satellite instrument. The algorithm is based on what has been used for polar-orbiting satellites and has been modified for application to geostationary satellites. The authors evaluate the retrieved NO_2 columns using TROPOMI and the operational GEMS retrievals and discuss the uncertainties in the retrievals.

This is a high-quality manuscript. It includes a complete description of the new algorithm and a thorough analysis of its strengths and weaknesses. It is well-written and makes good use of figures. I point out below a few points that could be better addressed.

1. The reader would benefit from a brief description of the operational GEMS algorithms near the beginning of the paper. It would help to include a table describing the major similarities and differences between the new and the operational GEMS algorithm.

Thanks for your suggestion. As the reviewer recommended, we will include Table 1 in Sect. 2 of the revised manuscript to summarize the main settings of the DLR GEMS and the operational v2.0 GEMS NO_2 algorithm.

Table 1. Overview of the GEMS tropospheric NO_2 retrievals from the DLR (this study) and GEMS operational v2 algorithm.

		DLR GEMS (this work)	GEMS operational v2.0 (Park et al., 2020)
Spectral fit settings for slant column retrievals	Fitting window	425 – 480 nm	432 - 450 nm
	Reference spectrum	Daily solar irradiance	Daily solar irradiance
	Absorption cross - sections	NO_2, O_3, H_2O_{vap}, H_2O_{liq}, O_4	NO_2, O_3, H_2O_{vap}, O_4
	Pseudo absorbers	Ring, Polarization sensitivity	Ring
	Polynomial	Fourth order	Second order
Stratosphere-troposphere separation		Stratospheric NO_2 estimation based on the CAMS forecast IFS Cy48R1 profile (detailed in Sect. 2.2.2)	Approach based on Bucsela et al. (2013)
Auxiliary input parameters for AMF calculations	Cloud parameter	Cloud fraction: OCRA adapted to GEMS Cloud pressure: GEMS cloud v2.0 (Kim et al., 2024)	Cloud fraction and pressure from GEMS cloud v2.0

	Surface albedo	GEMS BSR v2.0 (Sim et al., 2024)	GEMS BSR v2.0
	A priori NO_2 profile	CAMS forecast IFS Cy48R1 (Eskes et al., 2024)	Monthly mean hourly NO_2 profiles simulated from GEOS-Chem v13

2. The uncertainty analysis (Section 3.4) could be improved by discussing uncertainties specific to retrievals from geostationary satellites. For example, how do the retrieval uncertainties vary with the time of day, or how different are they near the edge of the field of view compared to the center?

In this study, the total uncertainty in tropospheric NO_2 vertical columns is derived through the uncertainty propagation, which is composed of slant column uncertainties, stratospheric column uncertainties, and tropospheric AMF uncertainties (described in Sect. 3.4 and Eq. 6 in the revised manuscript).

The most critical and challenging aspect of temporal variations in the expected total error in tropospheric NO_2 columns is the calculation of tropospheric AMF uncertainties. Important error sources are related to the a priori tropospheric profile shape, surface directional reflectance, and the cloud correction. Since the uncertainties in the tropospheric AMF depend on the uncertainty of the input parameter ($\sigma_{parameter}$) and the sensitivity of the AMF to each parameter ($\frac{\partial M}{\partial parameter}$), the accuracy of the error analysis is significantly affected by the precision of the auxiliary input data uncertainties. However, as mentioned in the manuscript, due to the lack of information on the uncertainties of GEMS auxiliary data products (i.e., GEMS surface albedo (GEMS BSR), GEMS cloud fraction and cloud pressure), typical fixed parameter uncertainties (σ_{α_s}= 0.02, σ_{p_c}= 50 hPa, σ_{f_c}= 0.05) used in previous TROPOMI studies were applied in this study. Therefore, we emphasize that a more precise analysis of total GEMS tropospheric NO_2 column uncertainties should be performed in the future once information on the GEMS auxiliary data uncertainties is available.

Despite the current limitations, we will add the following text about total uncertainty in GEMS tropospheric NO_2 columns for diurnal variation in Sect 3.4 (of the revised manuscript) as follows:

"In addition, the total uncertainty in GEMS tropospheric NO_2 columns varies with the scan hour (local time of the day). Generally, the total uncertainty is higher in polluted areas during the early morning rush hour. This is associated with a high peak-shaped profile near the surface due to increased traffic emissions within the lower atmospheric boundary layer. These shapes of a priori profiles for typical commuting hours lead to lower tropospheric AMFs (M_{tr}), resulting in higher total uncertainties in tropospheric NO_2 columns (see Eq. 6) compared to local noon.

Furthermore, for geostationary satellites observing from a fixed position, extreme viewing angles (near the edge of the scan) generally increase the slant column uncertainty due to higher spectral noise. However, this increased slant column uncertainty at large viewing geometries (high solar zenith angle and viewing zenith angle) does not always lead to higher total uncertainty in tropospheric NO_2, since the total uncertainty in tropospheric NO_2 column is also influenced by the tropospheric AMF, which varies not only with viewing geometry but also with other factors such as surface albedo and surface pressure."

3. The effect of aerosols on the NO_2 retrievals is important for Asia, and in most retrievals, it is considered implicitly in the cloud parameters retrieved using O2-O2 absorption. It is unclear whether the OCRA algorithm used in this work does the same. Does it instead correct for the presence of aerosols and could that partly explain why it retrieves lower cloud fractions (figures 9 and 10) compared to the GEMS retrieval?

As described in Sect. 2.3 and Table 1 (to be included in the revised manuscript), we used the cloud fraction from the OCRA algorithm (i.e., the operational TROPOMI (Loyola et al., 2018) and upcoming S4 cloud fraction retrieval algorithm) adapted to GEMS L1 data, and the cloud centroid pressure from the GEMS v2.0 L2 cloud product, which is based on the LUT approach using O_2-O_2 absorptions. The DLR cloud retrieval for cloud pressure with the ROCINN algorithm requires the Oxygen A-band in the NIR. Since this wavelength range is not covered by the GEMS instrument, we used the cloud pressure data from the GEMS v2.0 cloud product.

OCRA does not explicitly correct for the presence of aerosols. As for the parameters retrieved using the O_2-O_2 absorption, aerosols are also implicitly included in OCRA because OCRA retrieves a cloud fraction based on comparing the measured reflectance (irrespective if clouds or aerosols contribute to the reflectance) to the expected reflectance in fully clear and fully cloudy conditions. Hence, a very strong aerosol contamination could also be misinterpreted as a "false" cloud fraction by OCRA.

The differences seen for some clear scenes between OCRA and the GEMS cloud fraction product (see Fig. R1 below) are, to our understanding, more likely related to the different surface treatments in the two algorithms. According to Kim et al. (2024), the GEMS v2.0 cloud retrieval algorithm uses a monthly surface reflectance climatology from OMI as input, whereas OCRA uses a clear-sky climatology based on the EPIC instrument onboard the NASA DSCOVR platform. We found the surface features from OMI-based surface LER climatology (particularly for bright surfaces) get translated into the operational GEMS L2 cloud fraction product as shown in Fig. R1. This does not seem to be the case for OCRA when using the EPIC clear-sky climatology.

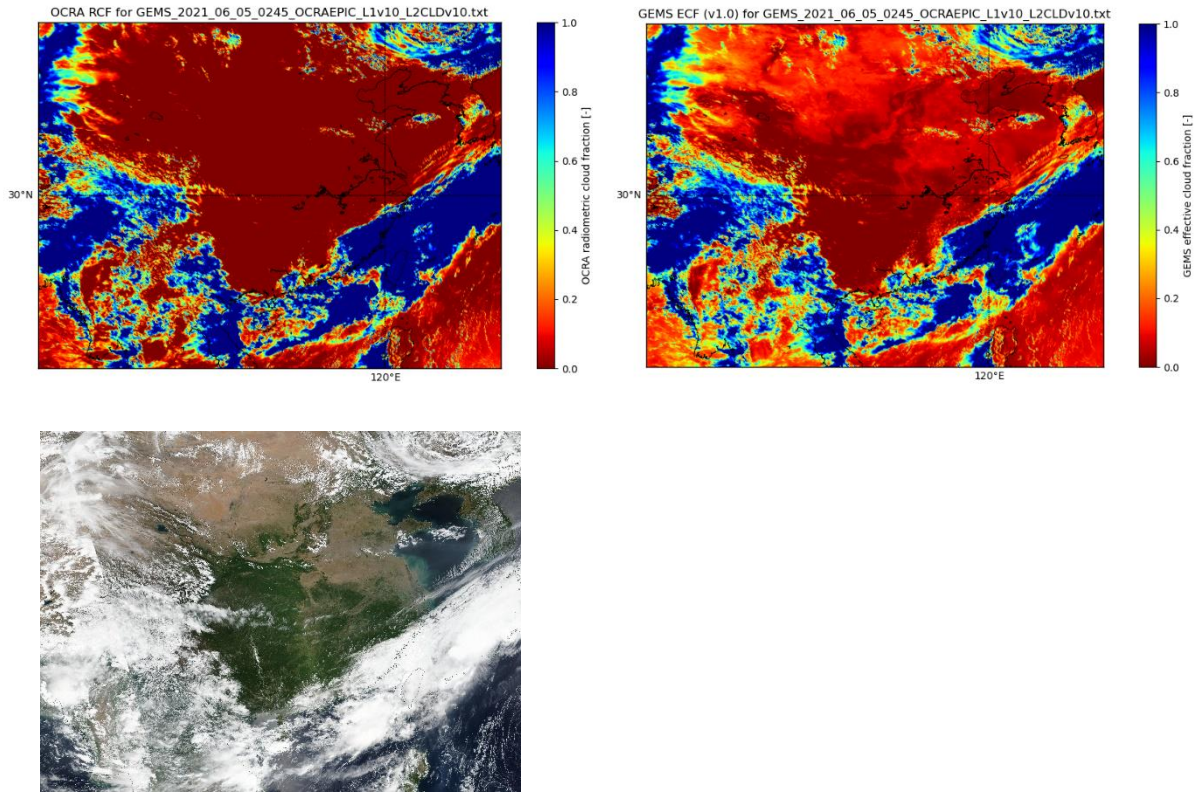

Figure R1. Zoom into a clear-sky region over China on the 2:45 UTC scan on 5 June 2021 for the OCRA cloud fraction (top left) and the operational GEMS v2.0 L2 cloud fraction (top right). The bottom left panel shows a true-colour RGB from VIIRS, taken from NASA Worldview. Note that the bright surface structures appearing in the northern part of the RGB true colour image seem to be translated into the operational GEMS cloud fraction product.

4. Equation 6: Is there an error correlation between albedo and cloud fraction (Boersma et al. 2018; doi: 10.5194/amt-11-6651-2018)?

In this study, as specified in Eq. (7) in Sect. 3.2 (revised version), we did not account for the contribution from the possible correlation between the cloud fraction and the surface albedo. We will consider the error correlation between cloud fractions and surface albedo in the tropospheric AMF uncertainty calculation in a follow-up study, using an improved version of GEMS surface albedo and cloud products and their uncertainties, which will be released in the near future.

5. Line 547-9: NO_2 is also photolyzed by visible radiation, not just UV. Another factor for the low noontime values of NO_2 is oxidation by OH.

Thank you for pointing out this. We revised the sentences (Line 547-549) as follows:

"During midday, given sufficient solar radiation, NO_2 is photolyzed to produce NO and oxygen atoms, and it is also oxidized by OH radicals, resulting in a decrease in tropospheric NO_2 levels."

References

Bucsela, E. J., Krotkov, N. A., Celarier, E. A., Lamsal, L. N., Swartz, W. H., Bhartia, P. K., Boersma, K. F., Veefkind, J. P., Gleason, J. F., and Pickering, K. E.: A new stratospheric and tropospheric NO 2 retrieval algorithm for nadir-viewing satellite instruments: applications to OMI, Atmos. Meas. Tech., 6, 2607–2626, https://doi.org/10.5194/amt-6-2607-2013, 2013.

Eskes, H., Tsikerdekis, A., Ades, M., Alexe, M., Benedictow, A. C., Bennouna, Y., Blake, L., Bouarar, I., Chabrillat, S., Engelen, R., Errera, Q., Flemming, J., Garrigues, S., Griesfeller, J., Huijnen, V., Ilic, L., Inness, A., Kapsomenakis, J., Kipling, Z., Langerock, B., Mortier, A., Parrington, M., Pison, I., Pitkanen, M., Remy, S., Richter, A., Schoenhardt, A., Schulz, M., Thouret, V., Warneke, T., Zerefos, C., and Peuch, V.-H.: Technical Note: Evaluation of the Copernicus Atmosphere Monitoring Service Cy48R1 upgrade of June 2023, EGUsphere [preprint], https://doi.org/10.5194/egusphere-2023-3129, 2024.

Kim, B.-R., Kim, G., Cho, M., Choi, Y.-S., and Kim, J.: First results of cloud retrieval from the Geostationary Environmental Monitoring Spectrometer, Atmos. Meas. Tech., 17, 453–470, https://doi.org/10.5194/amt-17-453-2024, 2024.

Loyola, D. G., Gimeno García, S., Lutz, R., Argyrouli, A., Romahn, F., Spurr, R. J. D., Pedergnana, M., Doicu, A., Molina García, V., and Schüssler, O.: The operational cloud retrieval algorithms from TROPOMI on board Sentinel-5 Precursor, Atmos. Meas. Tech., 11, 409–427, https://doi.org/10.5194/amt-11-409-2018, 2018.

Park, J., Lee, H., and Hong, H.: Geostationary Environment Monitoring Spectrometer (GEMS) Algorithm Theoretical Basis Document NO_2 Retrieval Algorithm, available at: https://nesc.nier.go.kr/ko/html/satellite/doc/doc.do (last access: 15 April 2024), 2020.

Sim, S., Choi, S., Jung, D., Woo, J., Kim, N., Park, S., Kim, H., Jeong, U., Hong, H., and Han, K.-S.: Retrieval pseudo BRDF-adjusted surface reflectance at 440 nm from Geostationary Environmental Monitoring Spectrometer (GEMS), EGUsphere [preprint], https://doi.org/10.5194/egusphere-2024-601, 2024.